

## ORIGINAL ARTICLE

# Linking phylogenetic and functional diversity to nutrient spiraling in microbial mats from Lower Kane Cave (USA)

Annette Summers Engel<sup>1</sup>, Daniela B Meisinger<sup>2</sup>, Megan L Porter<sup>3</sup>, Robert A Payn<sup>4</sup>, Michael Schmid<sup>5</sup>, Libby A Stern<sup>6</sup>, KH Schleifer<sup>2</sup> and Natuschka M Lee<sup>2</sup>

<sup>1</sup>Department of Geology and Geophysics, Louisiana State University, Baton Rouge, LA, USA; <sup>2</sup>Department of Microbiology, Technische Universität München, Freising, Germany; <sup>3</sup>Department of Biological Sciences, University of Maryland Baltimore County, Baltimore, MD, USA; <sup>4</sup>Department of Land Resources and Environmental Sciences, Montana State University, Bozeman, MT, USA; <sup>5</sup>Department Microbe-Plant Interactions, Helmholtz Zentrum München, German Research Center for Environmental Health (GmbH), Neuherberg, Germany and <sup>6</sup>FBI Laboratory Division, CFSRU, FBI Academy, Quantico, VA, USA

**Microbial mats in sulfidic cave streams offer unique opportunities to study redox-based biogeochemical nutrient cycles. Previous work from Lower Kane Cave, Wyoming, USA, focused on the aerobic portion of microbial mats, dominated by putative chemolithoautotrophic, sulfur-oxidizing groups within the *Epsilonproteobacteria* and *Gamma*proteobacteria. To evaluate nutrient cycling and turnover within the whole mat system, a multidisciplinary strategy was used to characterize the anaerobic portion of the mats, including application of the full-cycle rRNA approach, the most probable number method, and geochemical and isotopic analyses. Seventeen major taxonomic bacterial groups and one archaeal group were retrieved from the anaerobic portions of the mats, dominated by *Deltaproteobacteria* and uncultured members of the *Chloroflexi* phylum. A nutrient spiraling model was applied to evaluate upstream to downstream changes in microbial diversity based on carbon and sulfur nutrient concentrations. Variability in dissolved sulfide concentrations was attributed to changes in the abundance of sulfide-oxidizing microbial groups and shifts in the occurrence and abundance of sulfate-reducing microbes. Gradients in carbon and sulfur isotopic composition indicated that released and recycled byproduct compounds from upstream microbial activities were incorporated by downstream communities. On the basis of the type of available chemical energy, the variability of nutrient species in a spiraling model may explain observed differences in microbial taxonomic affiliations and metabolic functions, thereby spatially linking microbial diversity to nutrient spiraling in the cave stream ecosystem.**

*The ISME Journal* (2010) 4, 98–110; doi:10.1038/ismej.2009.91; published online 13 August 2009

**Subject Category:** geomicrobiology and microbial contributions to geochemical cycling

**Keywords:** subsurface; microbial mats; redox; nutrient spiraling; biogeochemistry; microbial diversity; geomicrobiology

## Introduction

Karst terrains extend over ~20% of the earth's surface (Ford and Williams, 2007), and caves are common features of karst terrains that allow study of subsurface habitats and ecosystems. Caves systems with surface entrances, but relative hydrological isolation from the surface, share basic physicochemical conditions, including complete darkness, year-round thermal stability, and relatively constant humidity.

Caves are also generally isolated from the influence of solar UV radiation and physical weathering due to wind, rain, or freezing. Compared to our understanding of biogeochemical cycling in photosynthetic microbial mats (Ferris *et al.*, 1997; Ward *et al.*, 1998), our knowledge of nutrient cycling in aphotic systems is limited, especially in the context of how nutrient cycling and microbial diversity might be linked. But, the redox-stratified microbial mats from a hydrogen sulfide (H<sub>2</sub>S)-bearing, anoxic to dysoxic cave stream habitat in Lower Kane Cave, Wyoming, USA (Figure 1), provide an opportunity to evaluate the relationships among habitat geochemistry, nutrient cycling, ecosystem function, and microbial diversity.

The microbial mats in Lower Kane Cave consist of filamentous and web-like morphotypes in contact with moving stream water. The filamentous surface

Correspondence: AS Engel, Department of Geology and Geophysics, Louisiana State University, Baton Rouge, LA 70803, USA. E-mail: aengel@lsu.edu or NM Lee, Department of Microbiology, Technische Universität München, 85354 Freising, Germany. E-mail: nlee@microbial-systems-ecology.de

Received 27 January 2009; revised 27 May 2009; accepted 8 July 2009; published online 13 August 2009

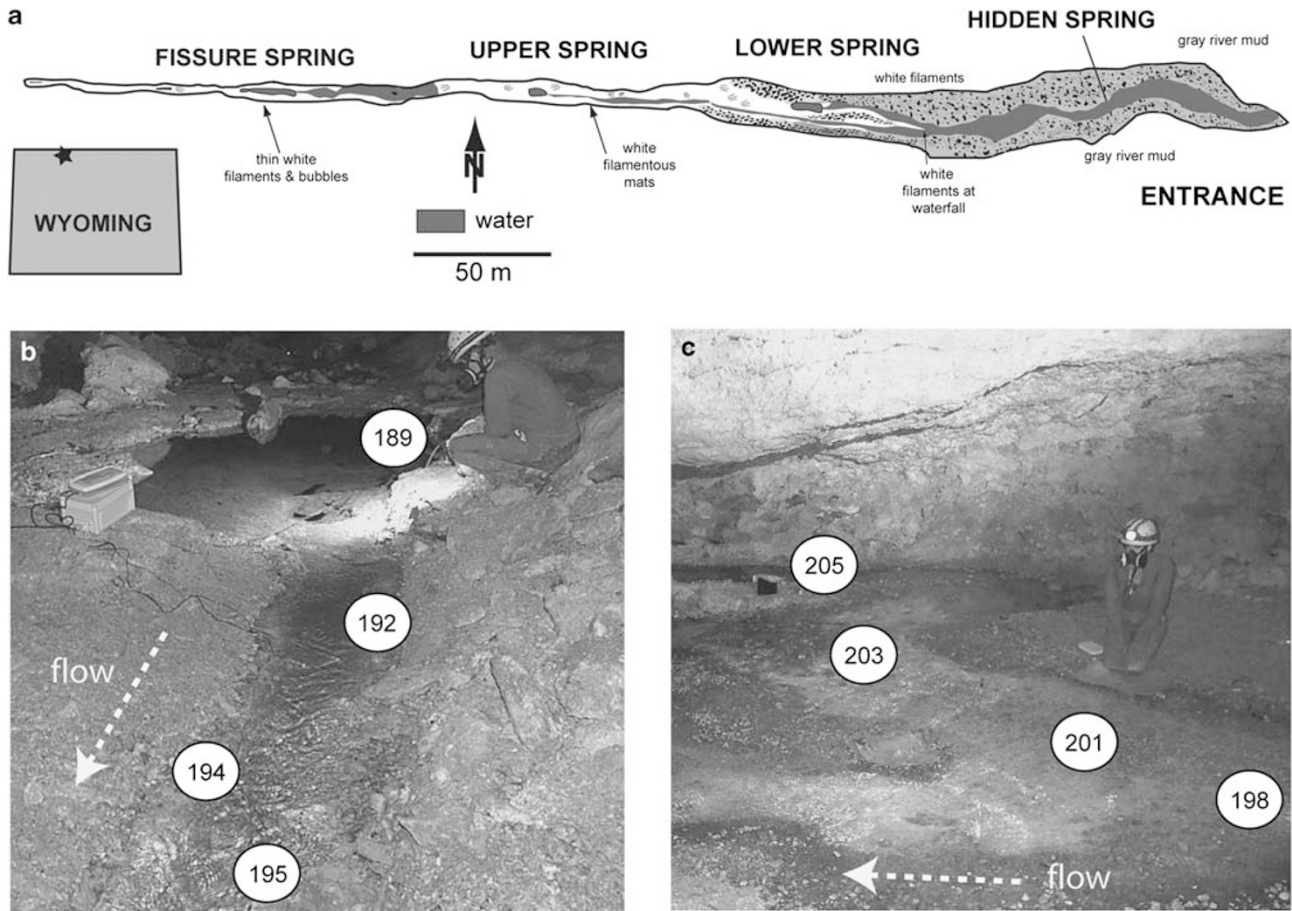


**Figure 1** (a) General cave location in Wyoming and plan-view cave map from Engel *et al.* (2004a). (b and c) Representative photographs from the Upper Spring transect, from the spring orifice (b) through the microbial mats downstream (c). Dashed arrows indicate flow direction. Numbers in circles represent sample locations, in meters.

covers a dense, gel-like mat interior. Dissolved oxygen profiles reveal that the first 3–5 mm of the mats are oxygenated, but that the mat interior is anoxic ( $\text{PO}_2 < 10 \text{ Pa}$ ) (Engel *et al.*, 2004a). Similar microbial mat and biofilm stratification has been reported recently from the Frasassi Caves in Italy (Macalady *et al.*, 2008). On the basis of the previous full-cycle rRNA investigations from Lower Kane Cave, the aerobic portions of the mats are dominated by uncultured representatives from the *Epsilon-proteobacteria* class and culturable representatives from *Thiothrix* spp. from the class *Gammaproteobacteria* (Engel *et al.*, 2003, 2004a). These groups form the bulk of the mats and provide chemolithoautotrophically fixed carbon and other nutrients to the ecosystem, but the diversity and dynamics of anaerobic microbial guilds, and their physical and functional relationships to aerobic groups, remain unknown.

In this study, we focused on the diversity, spatial arrangement, and abundance of anaerobic guilds to better evaluate ecosystem function and nutrient cycling in the microbial mats. We combined the

full-cycle 16S rRNA approach, including clone library construction and fluorescence *in situ* hybridization (FISH), with the most probable number (MPN) method to correlate to guild function. Stream water advection provided an opportunity to evaluate the oxidation state transformations between mobile (for example dissolved in moving stream water) and immobile (for example incorporated as relatively stationary biologic forms) dissolved solutes associated with abiotic and biotic processes. With the expanded view of microbial diversity, the nutrient spiraling concept (Webster and Patten, 1979) was evaluated using carbon and sulfur geochemical and stable isotope data. The distance of solute transport before biogeochemical transformation has been evaluated earlier in stream reaches through nutrient enrichment (Payn *et al.*, 2005) or transport-based analyses (Runkel, 2007), and has been used to describe nitrogen and phosphorus cycling and transport in surface stream ecosystems (Newbold *et al.*, 1981, 1982; Ensign and Doyle, 2006) and algal biofilms (Paul *et al.*, 1991), but to our knowledge this is the first time that nutrient spiraling has been

compared with the spatial patterns of aerobic and anaerobic microbial groups within aphotic microbial mats.

## Materials and methods

### *16S rRNA gene diversity and analyses*

The microbial diversity of the anaerobic portion of the mats was evaluated using earlier established methods to describe the aerobic portions of the mats (Engel *et al.*, 2003, 2004a; Meisinger *et al.*, 2007). Specific details regarding these methods, including sampling site information, geochemical analyses, DNA extraction, amplification, and sequencing, as well as FISH preparation and sample examination, and MPN estimations, are provided in the Supplementary material (abbreviated 'SM'). Nearly full-length (>1100 bp) 16S rRNA gene sequences from this study were proof-read and evaluated by the ARB software (Ludwig *et al.*, 2004), which consists of ~200 000 16S rRNA gene sequences that represent relevant relatives and outgroups to the retrieved clones according to BLAST searches in GenBank (<http://www.ncbi.nlm.nih.gov/>; Altschul *et al.*, 1990), the Ribosomal Database Project (RDP) (<http://rdp.cme.msu.edu/>; Cole *et al.*, 2007), and the SILVA databases (<http://www.arb-silva.de/>; Pruesse *et al.*, 2007). Chimeric clone sequences were identified by the ARB software using a partial treeing approach with two different filter sets that split the full-length sequence into two parts (for example *Escherichia coli* positions 1–750 and 751–1500) and performed separate treeing calculations on each section. If the two parts of the clone sequences were affiliated to different groups, then the sequences were identified as chimeric; ~10% of the sequences were identified as chimeric and were not included in further analyses. Nonchimeric sequences were submitted to GenBank under the accession numbers AM490641–AM490771.

Operational taxonomic units (OTUs) at the 98% similarity level were determined using DOTUR (Schloss and Handelsman, 2005). Coverage of the clone library was determined by rarefaction curves generated by aRarefactWin (Analytic Rarefaction ver. 1.3, <http://www.uga.edu/strata/software/software.html>). Sequences from the cave, close relatives, and outgroups were aligned by comparing select regions of the target gene sequences with alignment positions from multiple data sets (Ludwig *et al.*, 2004) and the resulting overall alignment was visually refined. A general phylogeny was reconstructed using the neighbour-joining distance method (Figure 2). For more refined analyses, sequences for major microbial groups were separated to reconstruct phylogenies using distance, maximum parsimony, and randomized a(x)ccelerated maximum likelihood methods (Stamatakis *et al.*, 2005). For each of these groups, a consensus tree was

constructed in ARB from all treeing procedures (Supplementary Figures SM1–SM10).

### *Distribution patterns from FISH and MPN counts*

Twenty-nine rRNA-targeted fluorescently labeled oligonucleotide probes were used for FISH to screen for different microbial groups present in 30 different mat samples distributed along the cave (Supplementary Table SM1). Although detection was limited to groups with at least  $10^5$  cells ml<sup>-1</sup> in the mats and a relatively high ribosome content (Schleifer, 2004), this approach allowed for screening major taxonomic groups from many different aerobic and anaerobic mat samples without generating clone libraries. Cultivable microbes capable of fermentation, sulfate reduction, sulfur reduction, iron reduction, nitrate-reducing sulfide oxidation, and methanogenesis were enumerated using the MPN method (Hurely and Roscoe, 1983). Details for each enrichment medium are included in the Supplementary material.

### *Assessment of nutrient cycling and spiraling*

Applicability of a nutrient spiraling model was evaluated using previous analyses of aqueous geochemistry and stable isotopes from cave stream waters and microbial mats (Engel *et al.*, 2004a, b). We focused on the Upper Spring transect, in which cave spring water had pH values of  $7.1 \pm 0.1$  and a nearly constant temperature of 21.5 °C. Stream velocity was previously determined from salt-dilution traces, which were approved in 2002 by the Bureau of Land Management as conservative and nondestructive to the microbial mats and cave ecosystem (which includes a federally endangered species); these restrictions currently limit use of radioactive or isotopic tracers. Engel *et al.* (2004b) measured dissolved and atmospheric gases to determine the theoretical  $C_T S^-$  concentrations in the cave stream if sulfide loss was due to (1) volatilization of gas-phase H<sub>2</sub>S from the cave stream and not considering turbulence, (2) autoxidation of  $C_T S^-$  along the stream reach (Engel *et al.*, 2004b), or (3) a net first-order loss of  $C_T S^-$  along the stream estimated from  $C_T S^-$  at the upstream and downstream ends of the reach:

$$\frac{C}{C_0} = e^{-kt} \quad (1)$$

where  $C$  is  $C_T S^-$  (shortened for clarity),  $C_0$  is  $C_T S^-$  at the upstream end of the reach,  $t$  is the transport time along the reach, and  $k$  is the first-order rate of  $C_T S^-$  transformation. Observed longitudinal distributions of  $C_T S^-$  were compared with the three simple models of sulfide loss listed above (volatilization, autoxidation, and net first-order loss). These comparisons were used to evaluate spatial variability in sulfide production and consumption along

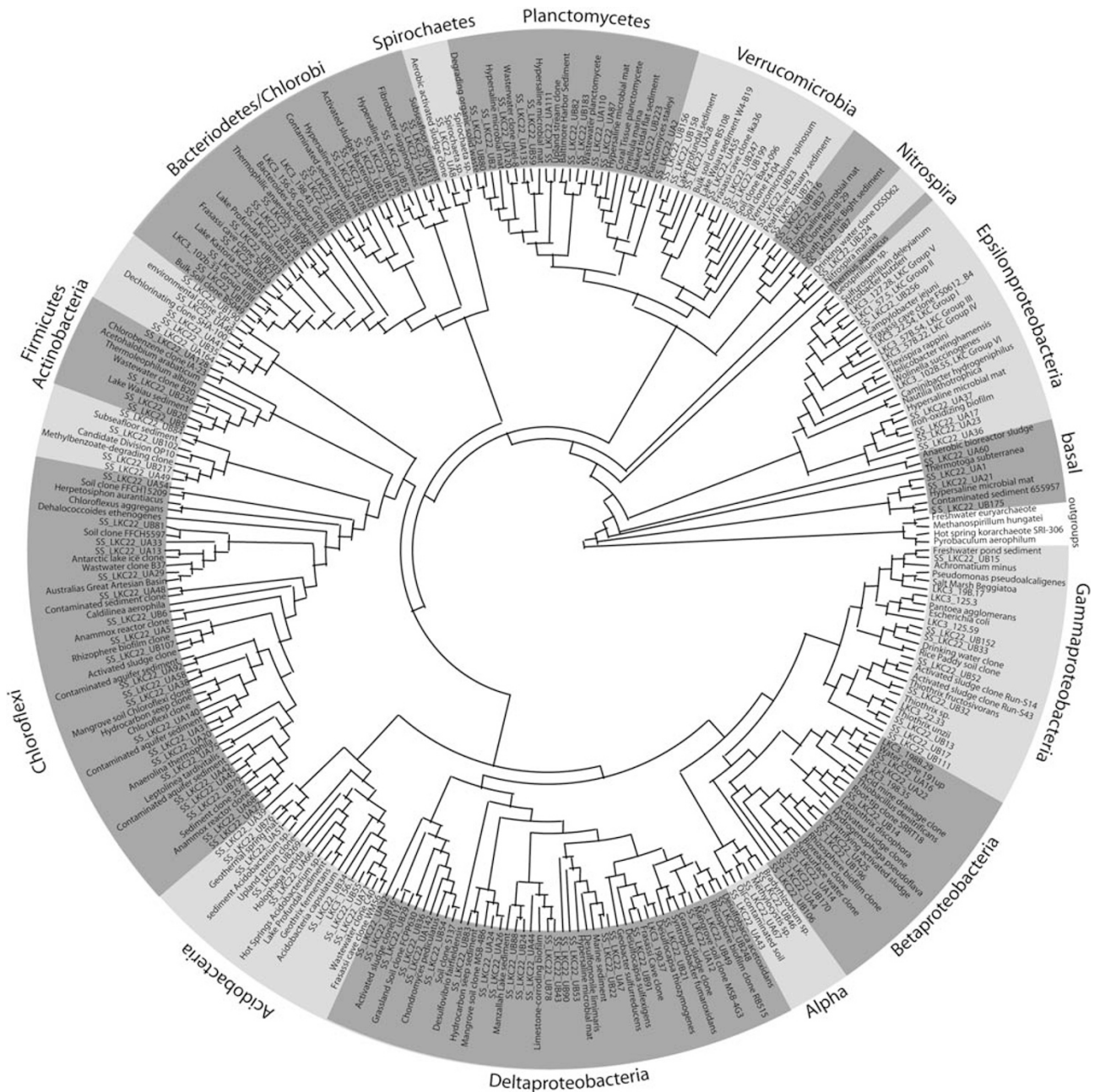


**Figure 2** Neighbor-joining phylogeny of 16S rRNA gene sequences ( $\geq 1100$  base pairs) from each of the representative bacterial taxonomic diversity from Lower Kane Cave and closest relatives. Major groups are indicated, and the tree was rooted using four archaeal sequences (AY822003, M60880, L07510, and AF255604).

the stream, and to compare these patterns to the microbial community structure and function.

## Results

### Microbial phylogenetic diversity

At least 17 major taxonomic bacterial groups and one archaeal group could be identified based on RFLP screening and partial (<600bp) 16S rRNA screening of all retrieved (346) clones from the 203 g mat sample (Figure 2; detailed results in Supple-

mentary Table SM2). Rarefaction estimates indicate that coverage barely approached saturation (Figure 3) and that the anaerobic mat community described by this work was more diverse than the aerobic mat samples reported earlier (Engel *et al.*, 2004a). Of the OTUs identified, only ~7% were  $\geq 98\%$  similar to previously identified groups in GenBank, corresponding to species-level relationships, and 122 novel OTUs were delineated based on 98% sequence identity. More than 50% of the clones were affiliated with three taxonomic groups: the *Delta*-*proteobacteria* ( $\delta$ -*Proteobacteria*), *Chloroflexi*, and

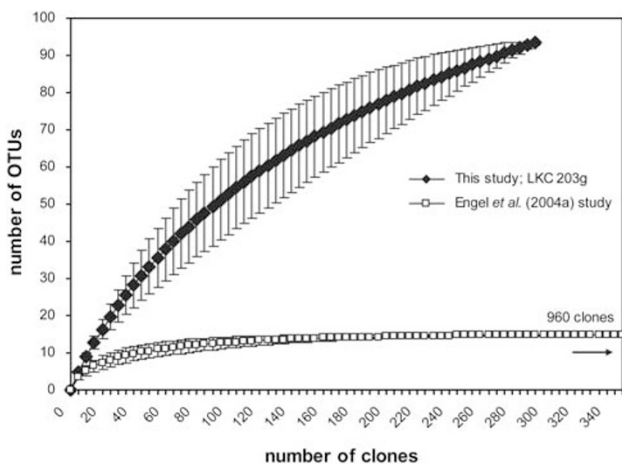


**Figure 3** Rarefaction curves based on operational taxonomic unit designation showing the diversity of the 203 g 16S rRNA gene sequence bacterial clone library from this study and of the clones from 10 libraries from the aerobic mat samples described in Engel *et al.* (2004a).

*Gammaproteobacteria* ( $\gamma$ -*Proteobacteria*). Nearly full-length sequences (>1100 bp) were retrieved for 135 representative clones for more detailed phylogenetic evaluation (Figure 2).

#### *Distribution and ecophysiology within the microbial mats*

As clone libraries do not provide distribution information (Juretschko *et al.*, 2002), FISH offered a more realistic view of the distribution and abundance of the dominant and tentatively active (that is with relatively high ribosome contents) groups identified by the clone library approach. Different levels of prokaryotic diversity were targeted with 29 oligonucleotide probes (Supplementary Table SM1), and all but 7 of the 29 probes yielded positive probe signals in at least one of the samples. No signals were observed using the probes targeting *Archaea* (Arch344), *Chloroflexi* (CFX1223 and GNSB941), nitrifying bacteria (Ntspa662 and Ntspa712), and *Verrucomicrobia* (EUBIII) (Table 1). Depending on the sample type, and of the 30 samples examined, *Bacteria* were detectable by FISH using the general EUB338mix probe for only 18 mat samples. Many of the samples were not suitable for FISH due to prevalent suspended or entrained inorganic material. Higher percentages of detectable cells could be identified by FISH in aerobic samples versus the anaerobic samples (Supplementary Figure SM11). Most of the aerobic and anaerobic mat samples analyzed had high abundances of six probe-targeted groups: the  $\gamma$ -*Proteobacteria*, *Epsilonproteobacteria* ( $\epsilon$ -*Proteobacteria*), *Acidobacteria*,  $\alpha$ -*Proteobacteria*,  $\delta$ -*Proteobacteria*, and the *Firmicutes* (Table 1; Supplementary Figure SM11). Filaments were the most targeted cell type, whereby positive signals were observed with probes for  $\epsilon$ -*Proteobacteria*,  $\delta$ -*Proteobacteria*,  $\gamma$ -*Proteobacteria*,  $\alpha$ -*Proteobacteria*, and

*Bacteroidetes*. The remaining probe-targeted groups were found in <30% of the investigated mat samples. As functional gene primers are not established for many possible metabolic lifestyles, construction of functional gene clone libraries would have been too time-consuming for the purposes of this study. Therefore, as a way to understand guild distribution in the microbial mats, MPN was used to screen and evaluate potentially lower abundance groups representing different metabolic life styles. Compared to the overall cell estimates of  $\sim 10^{10}$  cells ml<sup>-1</sup> from the aerobic portions of the mats based on cell carbon content (Engel *et al.*, 2004a), the MPN results enumerated five to six orders of magnitude less cells for each of the various anaerobic guilds (Figure 4).

Screening of the mat samples by FISH indicated that at least members affiliated to the  $\delta$ -*Proteobacteria* and *Firmicutes* were present (Table 1; Supplementary Figure SM11), and although the MPN results did not provide information regarding which sulfate-reducing microbial groups (abbreviated as SRP) were enriched, cell estimates for formatrophic and acetotrophic SRP were equally high (up to  $10^6$  cells ml<sup>-1</sup>) from almost all samples (Figure 4). Autotrophic SRP were not detected in all samples and generally had up to four orders of magnitude fewer cells. SRP cell abundance increased from the Upper Spring orifice downstream through the microbial mats. SRP were considerably less abundant in the cave stream (Figure 4). The aerobic and anaerobic mat samples had nearly equivalent SRP MPN estimates. Sulfate reduction is a polyphyletic metabolic process (Loy *et al.*, 2002), and although several lineages within the  $\delta$ -*Proteobacteria* class, the phyla *Thermodesulfobacteria*, *Nitrospirae* (for example *Thermodesulfobrevibrio*), *Firmicutes* (for example *Desulfotomaculum*), and some Archaea (for example *Archaeoglobus*) gain energy from sulfate reduction, FISH results indicated positive hybridization signals with the  $\delta$ -proteobacterial and *Firmicutes* probes in 70% of the mat samples (Table 1; Supplementary Figure SM11). *Firmicutes* represented  $\sim 7\%$  of the 16S rRNA gene clones, and none were related to known sulfate-reducers (for example, *Desulfotomaculum*) (Supplementary Table SM2). The majority of clones in the library was affiliated with the  $\delta$ -*Proteobacteria* related to environmental sequences retrieved from soil, sediments, the Frasassi Cave sulfidic stream microbial mats, and to cultured SRP like the filamentous *Desulfonema* spp., *Desulfomonile* spp., and *Chondromyces* spp. (Figure 2). S<sup>0</sup>RP taxonomic diversity is poorly known (Schauder and Kroger, 1993; Kletzin *et al.*, 2004; Kodama *et al.*, 2007). Several species are capable of disproportionating sulfur to sulfide and sulfate, including *Desulfocapsa thiozymogenes* (Finster *et al.*, 1998), which was retrieved in the clone library (Figure 2). Up to  $10^2$  S<sup>0</sup>RP cells ml<sup>-1</sup> were enumerated from MPN (Figure 4).

**Table 1** Summary of fluorescence *in situ* hybridization observations from microbial mat samples from Lower Kane Cave that were distinguished as aerobic (ae) and anaerobic (ana) mat types based on geochemistry

Probe-targeted group	Probes	Quality of probe signal	Cell morphologies observed	Number samples ae: ana	Distribution
<i>Bacteria</i>	EUB338	Weak to strong positive	Long+short rods; filaments; cocci	12:6	n.q.
<i>Acidobacteria</i>	Hol1400, 23S subd 7/8	Strong positive	Long+short rods	9:4	60%
<i>Actinobacteria</i>	HGC69a	Weak positive	Short rods	1:0	10%
<i>Bacteroidetes/Chlorobi</i>	CF319a,b,c	Strong positive	Long thin filaments; short rods	5:1	30%
<i>Firmicutes</i>	LGC354A,B,C	Weak positive	Long filaments; short rods	8:1	40%
<i>Planctomycetes</i>	EUB338-II/PLA46	Weak positive	Thin filaments	3:0	10%
<i>Alphaproteobacteria</i>	Alf 1b+968	Strong positive	Long filaments; short+long rods	10:2	40%
<i>Betaproteobacteria</i>	Bet42a+Gam42a comp	Weak positive	Long filaments	5:1	30%
<i>Deltaproteobacteria</i>	DELTA495a,b,c	Strong positive	Long filaments; short+long rods	9:3	40%
<i>Epsilonproteobacteria</i>	LKC1006; LKC59; EPSY549	Strong positive	Mainly long filaments	11:2	60%
<i>Gammaproteobacteria</i>	Gam42a+Bet42a comp	Strong positive	Long, wide filaments; short+long rods; cocci	11:7	70%
<i>Archaea</i>	Arch915, Arch344	Negative	n.d.	—	n.d.
<i>Chloroflexi</i>	CFX1223, GNSB941	Negative	n.d.	—	n.d.
<i>Nitrospirae</i>	Ntspa662/712	Negative	n.d.	—	n.d.
<i>Verrucomicrobia</i>	EUB338-III	Negative	n.d.	—	n.d.

The distribution of each probe-targeted group was estimated visually from all 30 microbial mat samples analyzed, and uncertainty is  $\sim \pm 10\%$ . Results for each sample are described on Supplementary Figure SM11. n.q., not quantifiable for all samples due to auto-fluorescence; n.d., no signal detected.

MPN revealed that fermenting microbes were present in 80% of the mat samples, at abundances up to  $10^6$  cells ml<sup>-1</sup> in the downstream samples (Figure 4). As fermentation is not limited to select taxonomic groups, different mixed-acid fermentation reactions were assessed (see Supplementary material). Of the 28 mixed-acid fermentation cultures, eight distinct types of heterotrophic growth were identified, predominately from downstream gray filament samples in which  $\sim 70\%$  of the mixed-acid fermentation enrichments produced acidity and CO<sub>2</sub> gas. Twenty-eight percent of the mixed-acid fermentation enrichments generated H<sub>2</sub>S. Ten percent of the enrichments grew on the TSI agar, but did not decrease medium pH or produce gas, suggesting one of four possibilities: (1) no fermentation; (2) fermentation but no decrease in pH or CO<sub>2</sub> production because of 2,3-butanediol or ethanol production; (3) only lactose fermentation; or (4) peptone catabolism. Hence, in addition to identifying different organic acid utilization pathways, we could also distinguish between butanediol and ethanol production that is common among Gram-positive bacteria like the *Firmicutes* (Talarico *et al.*, 2005), which represented 7% of the clone library. This group has not been found in high abundances from sulfidic cave systems previously, but it has been identified from cave-wall microbial communities and cave sediments (Laiz *et al.*, 2003; Schabereiter-Gurtner *et al.*, 2003; Cacchio *et al.*, 2004; Chelius and Moore, 2004; Ikner *et al.*, 2007).

Fourteen percent of the 16S rRNA gene sequence clones were related to uncultured *Chloroflexi* species (Figure 2; Supplementary Table SM2). Despite

*Chloroflexi* being retrieved from the Frasassi Caves (Engel *et al.*, 2007) and the H<sub>2</sub>S-bearing Zodletone Spring, Oklahoma (Elshahed *et al.*, 2003), the cave clones were more related to clones retrieved from soil, river sediments, or sludge (90–98% sequence similarity), and distantly related to cultured, anaerobic, filamentous strains (88–90% sequence similarity). FISH revealed that none of the microbial mats showed unambiguous positive hybridization signals to standard *Chloroflexi*-targeting fluorescently labeled probes (Table 1). However, preliminary studies using horse-radish peroxidase labeled *Chloroflexi* targeting probes (CFX 1223) and subsequent catalyzed reporter deposition-FISH (Pernthaler *et al.*, 2002) have recently revealed that a significant number of filamentous cells in the mats hybridized with this probe (Meisinger *et al.*, unpublished data). Because of their distant relationship to a large number of uncultured specimens found in anaerobic environments and to culturable nonobligate anaerobic species, like the novel candidate genera *Leptolinea* and *Caldilinea* in subclass I and VI of *Chloroflexi* (Kohnno *et al.*, 2002; Yamada *et al.*, 2005) (Supplementary Table SM2), it is plausible that the novel *Chloroflexi* groups have an anaerobic lifestyle.

The importance of sulfur-oxidizing bacterial groups to sulfuric acid speleogenesis has been made apparent (Engel *et al.*, 2004b; Macalady *et al.*, 2006). The  $\gamma$ -*Proteobacteria* are predominately affiliated with the filamentous and sulfur-oxidizing genera *Thiothrix* spp. and *Beggiatoa* spp., and these groups were retrieved from the clone libraries (Figure 2), and FISH revealed that 70% of all mats had positive hybridization signals with the  $\gamma$ -proteobacterial

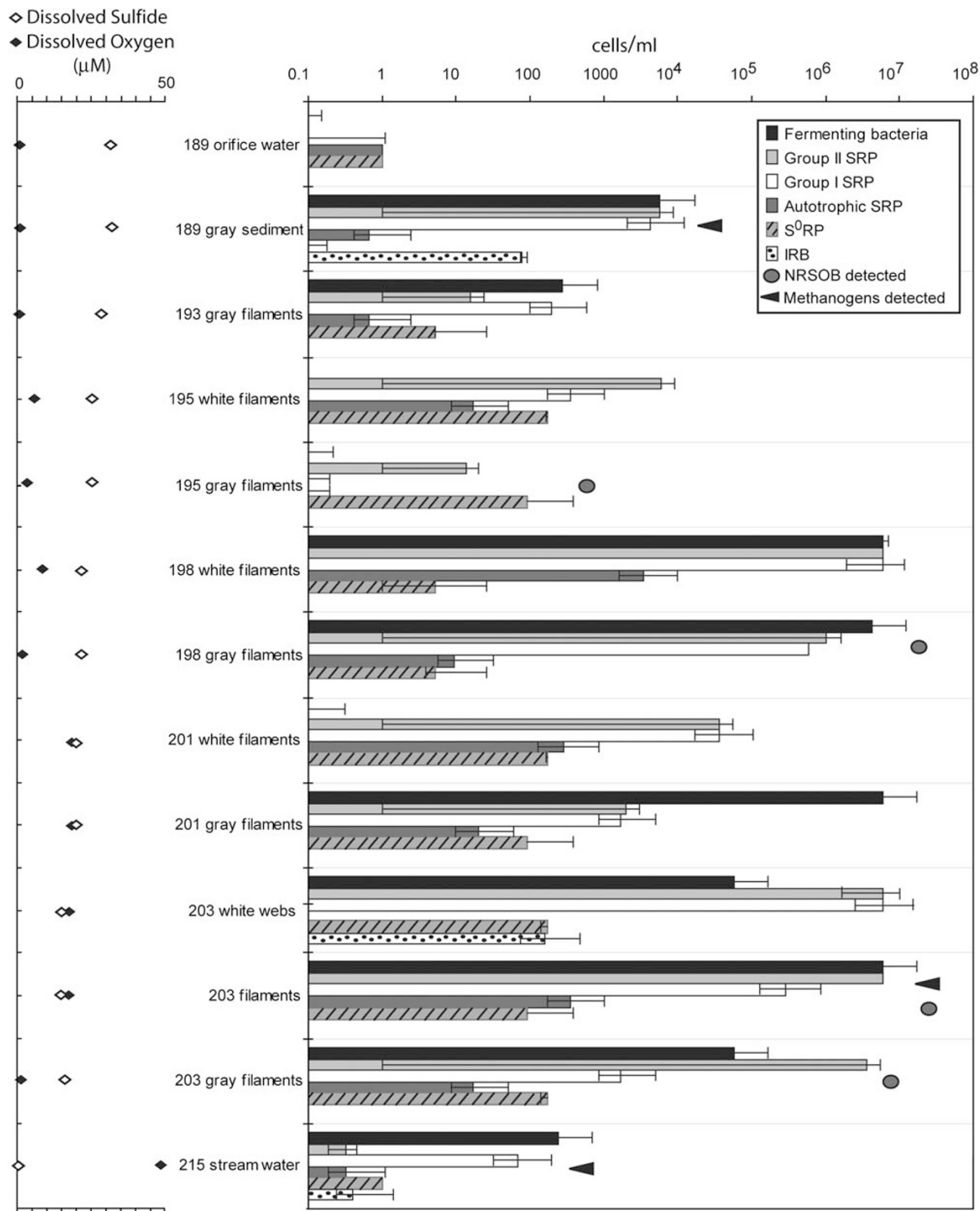


**Figure 4** Most probable number (MPN) estimates for anaerobic microbial guilds from Lower Kane Cave water, sediment, and microbial mat samples compared with dissolved oxygen and sulfide concentrations for each of those samples. Samples are along a transect of the Upper Spring (from 189 to 215 m). Number at left represents site location, in meters, from the back of the cave forward (the spring orifice is the lowest number). White mats are generally considered to be aerobic, while gray mats are anaerobic. SRP, sulfate-reducing prokaryotes (groups I and II, and autotrophic); S<sup>0</sup>RP, sulfur-reducing prokaryotes; DIRB, dissimilatory iron-reducing bacteria. Error bars are 95% confidence intervals calculated by the MPN program (Hurely and Roscoe, 1983). For nitrate-reducing sulfur-oxidizing bacteria (NRSOB) and methanogens, biomass estimates were not made and therefore only the presence of these groups is indicated; see text for methodological details.

probes, mostly to filaments, as well as to short and long rods and cocci (Table 1; Supplementary Figure SM11). The anaerobic metabolism of nitrate reduction linked to sulfide oxidation was evaluated by MPN. Half of the nitrate-reducing sulfide-oxidizing bacterial (NRSOB) enrichments had positive growth, predominately from the gray mat samples (Figure 4). As there are currently no FISH probes for this guild because the metabolism is polyphyletic, it was not possible to use FISH to identify NRSOB distribution patterns. But, 60% of the screened mat samples had positive signals for long filaments associated with the  $\epsilon$ -*Proteobacteria*, which could indicate the presence of NRSOB (Macalady *et al.*, 2006).

The remaining 16S rRNA clones represented a range of taxonomic and metabolic groups (Figure 2). None of the clones were closely related (>99% sequence identity) to known cultured organisms (Supplementary Table SM2). Nearly 10% of the clones were affiliated with Bacteroidetes/Chlorobi members that were related (89–98% similarity) to clones retrieved from lake, sludge, and tar-oil contaminated aquifers (Supplementary Table SM2). The Bacteroidetes/Chlorobi were only detected in downstream samples by FISH (Supplementary Figure SM11). Despite members of this large group being common in caves, including nonsulfidic examples, their functional role is generally poorly understood and attributed to fermentation or metal cycling (Angert *et al.*, 1998; Schabereiter-Gurtner *et al.*, 2003; Chelius and Moore, 2004; Macalady *et al.*, 2006; Ikner *et al.*, 2007). Up to  $10^3$  cells  $\text{ml}^{-1}$  of dissimilatory iron-reducing bacteria were identified from anaerobic sediment in the Upper Spring from MPN estimates, but were also detected from the aerobic mat samples downstream (Figure 4). None were detected from spring or stream water. Although Meisinger *et al.* (2007) hypothesized that some *Acidobacteria* may be capable of iron reduction, such as those distantly related to *Geothrix fermentans*, very few clones were retrieved that were closely related to known dissimilatory iron-reducing bacteria (Supplementary Table SM2). Cells hybridized with *Acidobacteria*-specific probes were detected by FISH in 60% of the samples, and in some instances, this was the most abundant group identified by FISH (Supplementary Figure SM11). Several of the remaining OTUs could not be assigned to a particular division, and given the low sequence identities (86–95%) it is possible that novel groups, even at the familial level, may exist due to affiliations with basal or unlabeled groups (Figure 2).

Diverse methanogens have been identified from  $\epsilon$ -*Proteobacteria*- and *Thiothrix*-dominated microbial mats from photic sulfidic springs (Moissl *et al.*, 2002; Elshahed *et al.*, 2004). However, there are strong indicators that methanogenic guilds have low population sizes in Lower Kane Cave, including trace detectable  $\text{CH}_4$  in the stream water (Engel

*et al.*, 2004a), low cell yields from MPN enrichments (Figure 4), low numbers of archaeal clones using three different primer pairs, and dubious fluorescent signals when using Archaea-specific FISH probes. All of the retrieved clones belonged to the *Euryarchaeota*, and were most closely related to a methanogenic freshwater sediment clone (Supplementary Table SM2). Interestingly, the rest of the clones amplified by PCR for *Archaea* were closely related to *Thiothrix* spp. FISH results were inconclusive for the *Archaea* because cell numbers may be too low to be detected by FISH, cell inactivity, or low ribosomal content, or because the *Archaea* probes, ARC344 and in particular Arch915, had unspecific probe signals to certain filaments. When Arch915 was combined with the  $\gamma$ -*Proteobacteria* probe Gam42a and *Thiothrix* spp.-specific probes, the filaments had overlapping signals. These results support several previous studies that indicate the present probe (Arch 915) and primer sets (A112f-A934b) used to target *Archaea* may yield erroneous (nonarchaeal) results (Amann and Fuchs, 2008).

#### *Sulfide dynamics and nutrient spiraling*

Spiraling metrics are typically based on travel distance along the stream (as defined by Newbold *et al.*, 1981), assuming an average influence of flow velocity on solute concentrations along a stream reach. Stream velocity was relatively constant from ~190 to 204 m at  $0.5 \text{ m s}^{-1}$ , but decreased to  $0.2 \text{ m s}^{-1}$  downstream of the microbial mat terminus (from ~204 to 219 m). We considered changes in  $C_T S^-$  relative to transport time to account for the distinct change in velocity, yielding a more traditional time-based kinetic model. We returned the time-based kinetic analyses to a variably scaled spatial spiraling context (Figure 5) to directly compare locations of  $C_T S^-$  processing and specific microbial guilds along the stream (Doyle, 2005). Although the concentrations of dissolved bicarbonate and sulfate did not vary appreciably along the cave stream, dissolved oxygen increased while  $C_T S^-$  values decreased (Figures 5b and c). The mats abruptly terminate between 203 and 204 m where dissolved oxygen exceeded  $45 \mu\text{mol l}^{-1}$  and  $C_T S^-$  was half the initial concentration (~28.7 s). From Equation (1),  $k$  was estimated as  $0.02 \text{ s}^{-1}$  from the difference between upstream and downstream  $C_T S^-$ . From 0 to 5 s, and beyond 30 s travel time, the observed  $C_T S^-$  values generally follow a first-order  $C_T S^-$  loss curve, although the observed values are slightly less than the expected values from 0 to 5 s (Figure 5c, black curve). Between 5 and 30 s, however, observed  $C_T S^-$  differed from the first-order loss curve. At any given dissolved oxygen concentration, the observed  $C_T S^-$  values were lower than would be expected for  $C_T S^-$  if loss was due to either autooxidation or volatilization processes (Figure 5c, gray curves) (Engel *et al.*, 2004b).

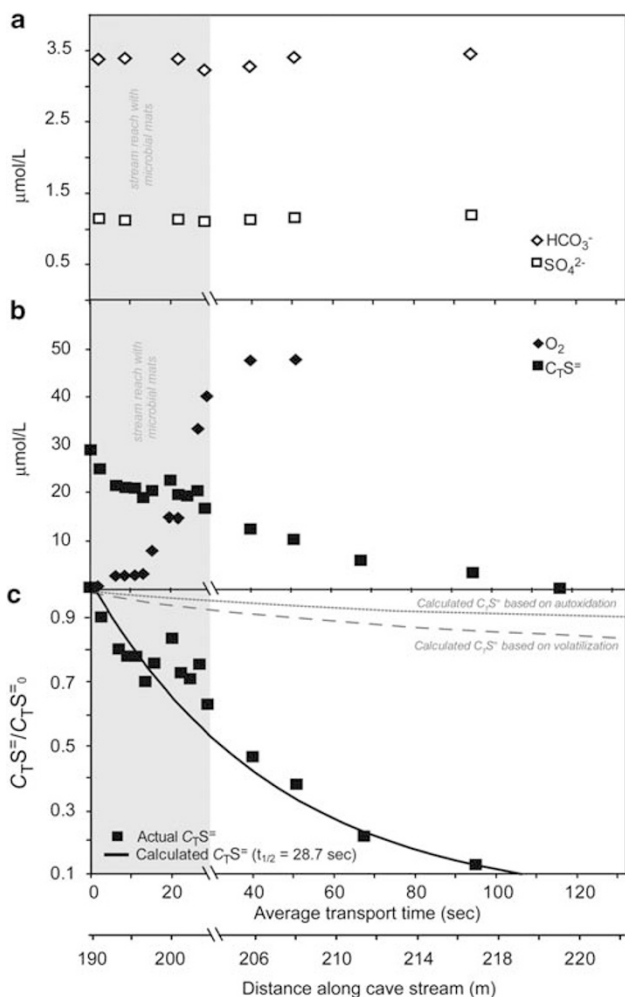


**Figure 5** (a) Dissolved bicarbonate and sulfate concentrations. (b) Dissolved oxygen and total dissolved sulfide ( $\text{C}_T\text{S}^=$ ) concentrations for the Upper Spring transect. (c) Observed  $\text{C}_T\text{S}^=$  versus modeled  $\text{C}_T\text{S}^= / \text{C}_T\text{S}^=_0$  based on a first-order loss from  $t_{1/2}$  of 28.7 s (black line), and on autooxidation and volatilization loss (gray lines) according to Engel *et al.* (2004b). The broken x axis indicates where there is a change in velocity. The shaded box in all panels denotes the stream reach with microbial mats (from 0 to ~30 s, or 190–204 m).

## Discussion

In the Lower Kane Cave stream system, the microbial mats are likely to alter the hydrodynamics of a system, increase the contact time of water and solutes with both aerobic and anaerobic portions of the mat, and thereby compress nutrient consumption and production spirals along the cave stream (Battin *et al.*, 2003). So, the susceptibility of a molecule to metabolic transformation, such as from a mobile to immobile phase, increases as solute transport into mats from the water column becomes limiting. Gas-phase nutrients, such as  $\text{H}_2\text{S}$ ,  $\text{O}_2$ , and  $\text{CO}_2$ , have the greatest potential to be limiting, and we hypothesized that the resulting variations in the uptake (consumption) and release (production) rates of these nutrients downstream should influence the

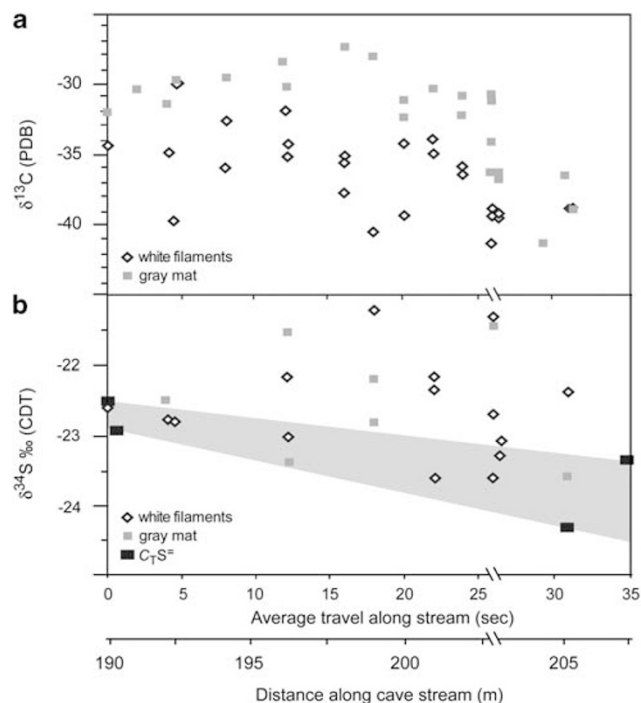


**Figure 6** (a) Carbon isotope compositions summarized from Engel *et al.* (2004a) for white (aerobic) and gray (anaerobic) filamentous microbial mat samples. (b) Sulfur isotope compositions for microbial biomass and the dissolved sulfide from the cave stream (Engel *et al.*, 2007). The broken x axis indicates a change in velocity.

longitudinal distribution of specific metabolic groups. We combined the full-cycle 16S rRNA approach with the MPN method to realize the physical and functional distribution of anaerobic microbial guilds and communities in the microbial mats. Our phylogenetic investigations uncovered the potential for undescribed biodiversity, and some groups have not been identified previously in subsurface systems. These results made evaluating the mechanisms that control changes in diversity difficult (Doebeli and Dieckmann, 2003; Mizera and Meszyna, 2003; Hansen *et al.*, 2007). But, the spatial distribution of microbial diversity was placed into a nutrient spiraling framework by interpreting hydrodynamic, geochemical, and biological processes that balance nutrient and energy flow along the cave stream (Webster and Patten, 1979; Newbold *et al.*, 1981, 1982; Runkel, 2007).

Consideration of stable carbon and sulfur isotope ratio analyses from the microbial mats and cave waters illustrate that nutrient spiraling influences changes in microbial diversity, and that a single net fractionation cannot be applied to the system due to the diversity of biological processes that offset the isotopic composition along stream (Figure 6). For Lower Kane Cave, chemolithoautotrophically fixed carbon serves as the trophic basis of this microbial ecosystem because photosynthetically produced carbon is unlikely to provide any significant energy to the system due to the cave's isolation from the

surface (Engel *et al.*, 2004a; Porter *et al.*, 2009). The  $\delta^{13}\text{C}$  values for microbial biomass are typical of autotroph-dominated biomass because they reflect the large, irreversible enzymatic discrimination against  $^{13}\text{C}$  from a dissolved inorganic carbon reservoir (Figure 6a). The dissolved inorganic carbon  $\delta^{13}\text{C}$  values decrease by  $\sim 2\%$  from the spring orifice (190 m) to the end of the mats at  $\sim 204$  m (Engel *et al.*, 2004a). Porter *et al.* (2009) indicate that at least 30% of the autotrophically fixed carbon in Lower Kane Cave microbial mats is cycled through a microbial detrital loop. From 0 to 10 s ( $\sim 190$ – $195$  m), where measured  $C_T\text{S}^-$  values are only slightly lower than expected (given experimental error) from the first-order loss curve (Figure 5c), the  $\delta^{13}\text{C}$  values for upstream samples, which consist predominately of  $\epsilon$ -*Proteobacteria* and few other groups (Supplementary Figure SM11), differ by  $< 5\%$  (Figure 6a). By  $\sim 16$ – $17$  s ( $\sim 197$  m), however, the differences between  $\delta^{13}\text{C}$  values from the white and gray mat samples increases to  $> 7\%$ . As excretion, respiration, and heterotrophic cycling of carbon should have negligible effects on carbon isotope values, the differences in  $\delta^{13}\text{C}$  values could be linked to changes in the abundances of different autotrophic  $\epsilon$ - and  $\gamma$ -proteobacterial groups and variations in the rates and expression of  $^{13}\text{C}$  discrimination during autotrophy (Engel *et al.*, 2004a). From 20 to 30 s ( $\sim 200$ – $205$  m), the white and gray  $\delta^{13}\text{C}$  biomass compositions are less variable, suggesting that the proximity of heterotrophs to autotrophically produced organic carbon may cause immediate sequestration of carbon rather than its downstream transport (Battin *et al.*, 2003). In other words, the biomass  $\delta^{13}\text{C}$  decreases with each carbon spiral along the stream because of a feedback effect between autotrophic fractionation (negative for  $^{13}\text{C}$ ) and the continual respiration of autotrophically fixed organic carbon from upstream. Carbon spiraling should homogenize the  $\delta^{13}\text{C}$  in the organic and inorganic carbon pools with increasing distance downstream, as well as cause the ensuing decrease in the  $\delta^{13}\text{C}$  dissolved inorganic carbon downstream, because  $\text{CO}_2$  respired upstream is used by downstream autotrophs.

The  $\delta^{34}\text{S}$  values for  $C_T\text{S}^-$  in the cave stream decrease by  $\sim 1.6\%$  along the cave stream, and white and gray biomass  $\delta^{34}\text{S}$  values are variable (Figure 6b). The gray mat samples from the middle of the stream have the highest abundance of sulfate-reducing and heterotrophic groups (Figure 4), and these samples also correspond to a reach where measured  $C_T\text{S}^-$  exceeds the first-order  $C_T\text{S}^-$  decay loss (Figure 5c). The increase in  $C_T\text{S}^-$  could not be due to abiotic processes, so the large and diverse community of SRP and fermenters are responsible for producing autochthonous sulfide. As autochthonous  $\text{H}_2\text{S}$  would have very low  $\delta^{34}\text{S}$  values compared with allochthonous dissolved sulfide in the cave stream, consumption of this autochthonous sulfide by sulfur-oxidizing community would shift

the average  $\delta^{34}\text{S}$  values for microbial biomass downstream by more than  $\pm 1\%$  (Fry *et al.*, 1988; Mandernack *et al.*, 2003). Differences in autochthonous  $\text{H}_2\text{S}$  uptake rates downstream, as well as differences in retention of sulfur-containing compounds within the mats downstream, may result in compositional variability. The mean sulfur content of white filaments is  $\sim 30\%$  w/w, whereas gray filaments only have  $\sim 2\%$  sulfur (Engel *et al.*, 2004a). In contrast, most cells have values approximately equal to 1% in the absence of stored sulfur (Fagerbakke *et al.*, 1996). Engel *et al.* (2007) confirmed that sulfur in white filaments is cyclo-octasulfur ( $\text{S}_8$ ), or elemental sulfur, which accumulates as a byproduct of sulfur oxidation, but that sulfur in the gray filaments is mostly as monosulfane from the accumulation of amino acids.

These correlations among microbial abundance and diversity,  $C_T\text{S}^-$  dynamics, and the isotopic composition of water and mats provide a basic understanding that nutrient spiral dimensions lengthen or shorten (that is loosen or tighten; Webster and Patten, 1979) in different segments of the stream, even if we do not yet fully understand uptake and turnover dynamics between the aerobic and anaerobic portions of the mats. For instance, it is possible that some groups may facultatively switch from autotrophy to mixotrophy as autochthonous organic carbon availability increases. Therefore, given the complexity of this natural system, future work will require a more detailed characterization of the hydrology (Doyle, 2005; Runkel, 2007), nutrient addition experiments, and the introduction of conservative hydrologic tracers to quantify how spiraling dimensions change with shifts in community composition and metabolism, or how biological or hydraulic retention influence spiral lengths due to reactive transport and nutrient retention and storage within the microbial mats. More detailed modeling of the system will also require characterizing gas ( $\text{H}_2\text{S}$ ) transfer across the stream–air interface, which is not implemented in the more commonly used active solute transport models (for example OTIS; Runkel, 1998). Lastly, microbial functional processes should also be explored and quantified, such as from functional genomics and expression studies.

In conclusion, this study expands the known diversity of some microbial groups to caves and the subsurface, even though the microbial diversity of various sulfidic caves and aquifers has been investigated for more than a decade (Sarbu *et al.*, 1996; Vlasceanu *et al.*, 1997, 2000; Hose *et al.*, 2000; Barton and Luiszer, 2005; Macalady *et al.*, 2006). In Lower Kane Cave, anaerobic mat communities were more taxonomically and metabolically diverse relative to the aerobic mat communities. Although groups like SRP and fermenters present a fraction of the whole cell abundance of the system, their metabolic impact is reflected and recorded in the geochemistry (that is isotopically) of the system.

Changes in the forms and abundances of nutrients influence the overall functional diversity with distance downstream, and this may result in the emergence of potentially specialized groups of differing genetic and functional compositions downstream (Battin *et al.*, 2003; Mizera and Meszner, 2003; Parnell *et al.*, 2009). Evaluation of carbon and sulfur nutrient spiraling in Lower Kane Cave improves our understanding of ecosystem function in aphotic habitats and will help us to understand microbial processes occurring in other modern, redox-stratified microbial mat systems.

## Acknowledgements

The Bureau of Land Management, Cody Office, granted permission for the work. Field assistance was given by PC Bennett, SA Engel, T Dogwiler, K Mabin, M Edwards, J Deans, and HH Hobbs, III. Partial funding was provided from the Department Geological Sciences of The University of Texas at Austin (to ASE), the Life in Extreme Environments (LEExEn) program of the NSF (EAR-0085576 to PC Bennett and LAS at The University of Texas at Austin), and from the Technische Universität München and the Helmholtz Foundation for the 'virtual institute for isotope biogeochemistry—biologically mediated processes at geochemical gradients and interfaces in soil—water systems' (to DBM and NML). Continued funding to ASE was provided by the College of Basic Sciences, Louisiana State University. Insightful contributions for the nutrient spiraling concept were provided by K Simon and H Bao, and valuable discussions were also provided by PC Bennett, M Wagner (University of Vienna), W Liebl and W Ludwig (both at TUM, Technische Universität München).

## References

- Altschul SF, Gish W, Miller W, Myers EW, Lipman DJ. (1990). Basic local alignment search tool. *J Mol Biol* **215**: 403–410.
- Amann R, Fuchs BM. (2008). Single-cell identification in microbial communities by improved fluorescence *in situ* hybridization techniques. *Nature Rev Microbiol* **6**: 339–348.
- Angert ER, Northup DE, Reysenbach A-L, Peek AS, Goebel BM, Pace NR. (1998). Molecular phylogenetic analysis of a bacterial community in Sulphur River, Parker Cave, Kentucky. *Am Mineral* **83**: 1583–1592.
- Barton HA, Luiszer F. (2005). Microbial metabolic structure in a sulfidic cave hot spring: potential mechanisms of biospeleogenesis. *J Cave Karst Stud* **67**: 28–38.
- Battin TJ, Kaplan LA, Newbold JD, Hansen CME. (2003). Contributions of microbial biofilms to ecosystem processes in stream mesocosms. *Nature* **426**: 439–442.
- Cacchio P, Contento R, Ercole C, Cappuccio G, Preite Martinez M, Lepidi A. (2004). Involvement of microorganisms in the formation of carbonate speleothems in the Cervo Cave (L'Aquila-Italy). *Geomicrobiol J* **21**: 497–509.
- Chelius MK, Moore JC. (2004). Molecular phylogenetic analysis of Archaea and bacteria in Wind Cave, South Dakota. *Geomicrobiol J* **21**: 123–134.
- Cole JR, Chai B, Farris RJ, Wang Q, Kulam-Syed-Mohideen AS, McGarrell DM *et al.* (2007). The ribosomal database project (RDP-II): introducing myRDP space and quality controlled public data. *Nucleic Acids Res* **35**: D169–D172.
- Doebeli M, Dieckmann U. (2003). Speciation along environmental gradients. *Nature* **421**: 259–264.
- Doyle MW. (2005). Incorporating hydrologic variability into nutrient spiraling. *J Geophys Res* **110**: G01003, doi:10.1029/2005JG000015.
- Elshahed MS, Najar FZ, Roe BA, Oren A, Dewers TA, Krumholz LR. (2004). Survey of archaeal diversity reveals an abundance of halophilic Archaea in a low-salt, sulfide- and sulfur-rich spring. *Appl Environ Microbiol* **70**: 2230–2239.
- Elshahed MS, Senko JM, Najar FZ, Kenton SM, Roe BA, Dewers TA *et al.* (2003). Bacterial diversity and sulfur cycling in a mesophilic sulfide-rich spring. *Appl Environ Microbiol* **69**: 5609–5621.
- Engel AS, Lee N, Porter ML, Stern LA, Bennett PC, Wagner M. (2003). Filamentous 'Epsilonproteobacteria' dominate microbial mats from sulfidic cave springs. *Appl Environ Microbiol* **69**: 5503–5511.
- Engel AS, Lichtenberg H, Prange A, Hormes J. (2007). Speciation of sulfur from filamentous microbial mats from sulfidic cave springs using X-ray absorption near-edge spectroscopy. *FEMS Microbiol Lett* **269**: 54–62.
- Engel AS, Porter ML, Stern LA, Quinlan S, Bennett PC. (2004a). Bacterial diversity and ecosystem function of filamentous microbial mats from aphotic (cave) sulfidic springs dominated by chemolithoautotrophic 'Epsilonproteobacteria'. *FEMS Microbiol Ecol* **51**: 31–53.
- Engel AS, Stern LA, Bennett PC. (2004b). Microbial contributions to cave formation: new insight into sulfuric acid speleogenesis. *Geology* **32**: 369–372.
- Ensign SH, Doyle MW. (2006). Nutrient spiraling in streams and river networks. *J Geophys Res* **111**: G04009; doi:10.1029/2005JG000114.
- Fagerbakke KM, Heldal M, Norland S. (1996). Content of carbon, nitrogen, oxygen, sulfur, and phosphorous in native aquatic and cultured bacteria. *Aq Microbiol Ecol* **10**: 15–27.
- Ferris MJ, Nold SC, Revsbech NP, Ward DM. (1997). Population structure and physiological changes within a hot spring microbial mat community following disturbance. *Appl Environ Microbiol* **63**: 1367–1374.
- Finster K, Liesack W, Thamdrup B. (1998). Elemental sulfur and thiosulfate disproportionation by *Desulfocapsa sulfoexigens* sp. nov., a new anaerobic bacterium isolated from marine surface sediment. *Appl Environ Microbiol* **64**: 119–125.
- Ford DC, Williams P. (2007). *Karst Geomorphology and Hydrology*. J Wiley & Sons, Inc.: Sussex, pp 576.
- Fry B, Ruf W, Gest H, Hayes JM. (1988). Sulfur isotope effects associated with oxidation of sulfide by O<sub>2</sub> in aqueous solution. *Chem Geol* **73**: 205–210.
- Hansen SK, Rainey PB, Haagensen JAJ, Molin S. (2007). Evolution of species interactions in a biofilm community. *Nature* **445**: 533–536.
- Hose LD, Palmer AN, Palmer MV, Northup DE, Boston PJ, DuChene HR. (2000). Microbiology and geochemistry in a hydrogen-sulphide rich karst environment. *Chem Geol* **169**: 399–423.

- Hurely MA, Roscoe ME. (1983). Automated statistical analysis of microbial enumeration by dilution series. *J Appl Bacteriol* **55**: 157–164.
- Ikner LA, Toomey RS, Nolan G, Neilson JW, Pryor BM, Maier RM. (2007). Culturable microbial diversity and the impact of tourism in Kartchner Caverns, Arizona. *Microbial Ecol* **53**: 30–42.
- Juretschko S, Loy A, Lehner A, Wagner M. (2002). The microbial community composition of a nitrifying-denitrifying activated sludge from an industrial sewage treatment plant analyzed by the full-cycle rRNA approach. *System Appl Microbiol* **25**: 84–99.
- Kletzin A, Urich T, Müller F, Bandejas TM, Gomes CM. (2004). Dissimilatory oxidation and reduction of elemental sulfur in thermophilic archaea. *J Bioenerg Biomembr* **36**: 77–91.
- Kodama Y, Ha LT, Watanabe K. (2007). *Sulfurospirillum cavolei* sp. nov., a facultatively anaerobic sulfur-reducing bacterium isolated from an underground crude oil storage cavity. *Int J Syst Evol Microbiol* **57**: 827–831.
- Kohno T, Sei K, Mori K. (2002). Characterization of Type 1851 organism isolated from activated sludge samples. *Water Sci Technol* **46**: 111–114.
- Laiz L, Gonzalez-Delvalle M, Hermosin B, Ortiz-Martinez A, Saiz-Jimenez C. (2003). Isolation of cave bacteria and substrate utilization at different temperatures. *Geomicrobiol J* **20**: 479–489.
- Loy A, Lehner A, Lee N, Adamczyk J, Meier H, Ernst J *et al.* (2002). Oligonucleotide microarray for 16S rRNA gene-based detection of all recognized lineages of sulfate-reducing prokaryotes in the environment. *Appl Environ Microbiol* **68**: 5064–5081.
- Ludwig W, Strunk O, Westram R, Richter L, Meier H, Yadhukumar *et al.* (2004). ARB: a software environment for sequence data. *Nucleic Acids Res* **32**: 1363–1371.
- Macalady JL, Dattagupta S, Schaperdorth I, Jones DS, Druschel GK, Eastman D. (2008). Niche differentiation among sulfur-oxidizing bacterial populations in cave waters. *ISME J* **2**: 590–601.
- Macalady JL, Lyon EH, Koffman B, Albertson LK, Meyer K, Galdenzi S *et al.* (2006). Dominant microbial populations in limestone-corroding stream biofilms, Frasassi Cave system, Italy. *Appl Environ Microbiol* **72**: 5596–5609.
- Mandernack KW, Krouse HR, Skei JM. (2003). A stable sulfur and oxygen isotopic investigation of sulfur cycling in an anoxic marine basin, Framvaren Fjord, Norway. *Chem Geol* **195**: 181–200.
- Meisinger DB, Zimmermann J, Ludwig W, Schleifer K-H, Wanner G, Schmid M *et al.* (2007). *In situ* detection of novel *Acidobacteria* in microbial mats from a chemo-lithoautotrophically based cave ecosystem (Lower Kane Cave, WY, USA). *Environ Microbiol* **9**: 1523–1534.
- Mizera F, Meszena G. (2003). Spatial niche packing, character displacement and adaptive speciation along an environmental gradient. *Evol Ecol Res* **5**: 363–382.
- Moissl C, Rudolph C, Huber R. (2002). Natural communities of novel *Archaea* and bacteria with a string-of-pearls-like morphology: molecular analysis of the bacterial partners. *Appl Environ Microbiol* **68**: 933–937.
- Newbold JD, Elwood JW, O'Neill RV, Van Winkle W. (1981). Measuring nutrient spiraling in streams. *Can J Fish Aquat Sci* **38**: 860–863.
- Newbold JD, Mulholland PJ, Elwood JW, O'Neill RV. (1982). Organic carbon spiraling in stream ecosystems. *Oikos* **38**: 266–272.
- Parnell JJ, Crowl TA, Weimer BC, Pfrender ME. (2009). Biodiversity in microbial communities: system scale patterns and mechanisms. *Mol Eco* **18**: 1455–1462; doi: 10.1111/j.1365-294X.2009.04128.x.
- Paul BJ, Duthie HC, Taylor WD. (1991). Nutrient cycling by biofilms in running waters of differing nutrient status. *J North Am Benthol Soc* **10**: 31–41.
- Payn RA, Webster JR, Mulholland PJ, Valett HM, Dodds WK. (2005). Estimation of stream nutrient uptake from nutrient addition experiments. *Limnol Oceanogr Meth* **3**: 174–182.
- Pernthaler A, Pernthaler J, Amann R. (2002). Fluorescence *in situ* hybridization and catalyzed reporter deposition for the identification of marine bacteria. *Appl Environ Microbiol* **68**: 3094–3101.
- Porter ML, Engel AS, Kane TC, Kinkle BK. (2009). Productivity-diversity relationships from chemo-lithoautotrophically based sulfidic karst systems. *Int J Speleol* **3**: 27–40.
- Pruesse E, Quast C, Knittel K, Fuchs B, Ludwig W, Peplies J *et al.* (2007). SILVA: a comprehensive online resource for quality checked and aligned ribosomal RNA sequence data compatible with ARB. *Nucleic Acid Res* **35**: 7188–7196.
- Runkel RL. (1998). One dimensional transport with inflow and storage (OTIS): a solute transport model for streams and rivers. U.S. Geological Survey Water-Resources Investigations Report 98-4018. US Geological Survey, Denver, Colorado (<http://co.water.usgs.gov/otis>).
- Runkel RL. (2007). Toward a transport-based analysis of nutrient spiraling and uptake in streams. *Limnol Oceanogr Meth* **5**: 50–62.
- Sarbu SM, Kane TC, Kinkle BK. (1996). A chemoautotrophically based cave ecosystem. *Science* **272**: 1953–1955.
- Schabereiter-Gurtner C, Saiz-Jimenez C, Piñar G, Lubitz W, Rölleke S. (2003). Phylogenetic diversity of bacteria associated with Paleolithic paintings and surrounding rock walls in two Spanish caves (Llonín and La Garma). *FEMS Microbiol Ecol* **1606**: 1–13.
- Schauder R, Kroger A. (1993). Bacterial sulfur respiration. *Arch Microbiol* **195**: 491–497.
- Schleifer K-H. (2004). Microbial diversity: facts, problems and prospects. *System Appl Microbiol* **27**: 3–9.
- Schloss PD, Handelsman J. (2005). Introducing DOTUR, a computer program for defining operational taxonomic units and estimating species richness. *Appl Environ Microbiol* **71**: 1501–1506.
- Stamatakis AP, Ludwig T, Meier H. (2005). RAxML-II: a program for sequential, parallel & distributed inference of large phylogenetic trees. *Concurrency Comp Practice Exp* **17**: 1705–1723.
- Talarico LA, Gil MA, Ingram LO, Maupin-Furlow JA. (2005). Construction and expression of an ethanol production operon in gram-positive bacteria. *Microbiol* **151**: 4023–4031.
- Vlasceanu L, Popa R, Kinkle B. (1997). Characterization of *Thiobacillus thioparus* LV43 and its distribution in a chemoautotrophically based groundwater ecosystem. *Appl Environ Microbiol* **63**: 3123–3127.
- Vlasceanu L, Sarbu SM, Engel AS, Kinkle BK. (2000). Acidic cave-wall biofilms located in the Frasassi Gorge, Italy. *Geomicrobiol J* **17**: 125–139.

- Ward DM, Ferris MJ, Nold SC, Bateson MM. (1998). A natural view of microbial biodiversity within hot spring cyanobacterial mat communities. *Microbiol Mol Biol Rev* **62**: 1353–1370.
- Webster JR, Patten BC. (1979). Effects of watershed perturbation on stream potassium and calcium dynamics. *Ecol Mono* **19**: 51–72.
- Yamada T, Sekiguchi Y, Imachi H, Kamagata Y, Ohashi A, Harada H. (2005). Diversity, localization, and physiological properties of filamentous microbes belonging to *Chloroflexi* subphylum I in mesophilic and thermophilic methanogenic sludge granules. *Appl Environ Microbiol* **71**: 7493–7503.

Supplementary Information accompanies the paper on The ISME Journal website (<http://www.nature.com/ismej>)